Threshold height $(h'F)_c$ for the meridional wind to play a deterministic role in the bottom side equatorial spread F and its dependence on solar activity

N. Jyoti, C. V. Devasia, R. Sridharan, and Diwakar Tiwari

Space Physics Laboratory, Vikram Sarabhai Space Centre, Trivandrum, India

Received 9 January 2004; revised 14 April 2004; accepted 27 May 2004; published 25 June 2004.

[1] Detailed investigations have been carried out on the occurrence of bottom side Equatorial Spread F (ESF) and the thermospheric meridional wind characteristics just before the former's initiation using ground based ionospheric data corresponding to the equinoctial periods of 1993–1998, from Trivandrum (8.5°N, 76.5°E, dip = 0.5°N) and Sriharikota (13.7°N, 80.2°E, dip ~ 10°N) in the Indian longitudes. Critical analysis of the base height of the F-region h′F at the time of triggering of ESF and the polarity of the meridional winds revealed that, if the h′F is above a certain level ESF occurred under both equatorward and poleward wind conditions. Below that level, ESF occurred only when equatorward winds were present implying that the equatorward winds must somehow be able to offset the reduced growth rate of the plasma instability responsible for ESF. A plausible explanation linking Equatorial Ionization Anomaly (EIA) and the consequent Equatorial Temperature and Wind Anomaly (ETWA) and the consequent neutral dynamics effectively enabling the instability even at lower height has been offered. The threshold height $(h'F)_c$ gleaned out on the basis of the polarity of the meridional winds has been shown to bear a linear relation to the solar activity and sheds light on the enigmatic short and long term variability of ESF. *INDEX TERMS:* 2411 Ionosphere: Electric fields (2712); 2431 Ionosphere: Ionosphere/magnetosphere interactions (2736); 2437 Ionosphere: Ionospheric dynamics; 2471 Ionosphere: Plasma waves and instabilities. **Citation:** Jyoti, N., C. V. Devasia, R. Sridharan, and D. Tiwari (2004), Threshold height $(h'F)_c$ for the meridional wind to play a deterministic role in the bottom side equatorial spread F and its dependence on solar activity, *Geophys. Res. Lett.*, *31*, L12809, doi:10.1029/2004GL019455.

1. Introduction

[2] The nighttime equatorial F-region is often characterized by the presence of plasma density irregularities of scale sizes ranging from a few centimeters to several hundred kilometers, referred to as Equatorial Spread F (ESF). The ESF develops only in the post sunset hours in the equatorial belt of ±20° dip latitude and manifests itself as bottom side spread in ionograms, plumes in the UHF/VHF and HF radars, ionospheric scintillations of VHF and UHF and as airglow intensity bite outs. The ESF is known to vary with season, local time, geographical location, and also with solar activity and all these aspects have been extensively covered in the literature [*Chandra and Rastogi*, 1972; *Woodman and LaHoz*, 1976; *Sastri et al.*, 1979a, 1979b; *Fejer and Kelley*, 1980; *Rastogi*, 1980; *Abdu et al.*, 1981, 1992; *Aarons*, 1993; *Subbarao and Krishnamurthy*, 1994; *Sultan*, 1996; *Basu and Coppi*, 1999; *Fejer et al.*, 1999; *Sahai et al.*, 2000; *Hysell and Burcham*, 2002; *Huang et al.*, 2002]. A comprehensive understanding of this phenomenon under varying solar and geophysical conditions is extremely important with our increased dependence on satellite based communications and Geodesy. It is known that, ESF is an outcome of Rayleigh-Taylor (R-T) instability in the equatorial ionosphere which in turn is controlled by both ionospheric and neutral atmospheric parameters like plasma density scale length (L), ion neutral collision frequency (ν_{in}) and neutral winds in addition to the main driving factor viz; the gravity (g). The generalized expression for the local growth rate of the R-T instability is given as [*Sekar and Raghavarao*, 1987; *Kelley*, 1989]

$$\gamma = \frac{1}{L}\left[\frac{g}{\nu_{in}} + \frac{E_x}{B} + W_x\left(\frac{\nu_{in}}{\Omega_i}\right) - W_z\right] \quad (1)$$

where W_x and W_z are the zonal winds and vertical winds respectively and E_x is the zonal electric field in the F-region, B is the geomagnetic field and Ω_i is the ion-gyro frequency.

[3] For a realistic estimate of the growth rate of the R-T instability one should take into account the field line integrated ionospheric conductivity extending from the F-region to the E-region, as it loads the F-region zonal electric fields (E_x) and hence the post sunset F-layer height rise [*Sultan*, 1996]. At lower heights, the growth rate of the instability would decrease due to the increased ν_{in}. For a simplistic case of slab geometry when the contribution to the integrated conductivity from the conjugate E-regions is not very significant, the overhead equatorial values approximate the field line integrated values [*Hanson et al.*, 1986] and only the instantaneous local effects need to be considered. Once triggered, the generalized R-T instability grows nonlinearly and the background conditions become important for further growth and sustenance. In addition, ESF is known to depend considerably on solar and geomagnetic activity. The former has to be understandably through the changes brought about in the background ionospheric and thermospheric parameters while the latter is essentially through the induced electrodynamical and neutral dynamical effects [*Chandra and Rastogi*, 1972; *Abdu*, 2001; *Sastri et al.*, 2004].

[4] In spite of a broader understanding of all these aspects, the day-to-day variability of ESF in a given season and solar epoch still remains an enigma. The present communication addresses to this important aspect. Herein

0094-8276/04/2004GL019455$05.00

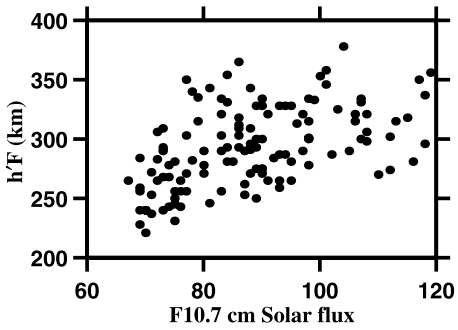

Figure 1. Variations of h′F corresponding to the time just before the onset of ESF on each day as a function of the F10.7 cm solar flux. A positive correlation with a linear trend is clearly seen in the h′F variations.

we restrict ourselves only to the study of bottom side spread F as seen in ground based ionograms and investigate the role of meridional neutral winds in offering a viable explanation for the observed variability.

[5] The effects of meridional winds on the occurrence of bottomside spread F was first studied by *Maruyama* [1988] and later supported by *Mendillo et al.* [1992] wherein they concluded that transequatorial poleward winds would inhibit ESF by pushing the F-region ionization to lower heights along the magnetic field lines away from the dip equator, enhancing the field line integrated conductivities and, the consequent loading of the F-region dynamo that is primarily responsible for the post sunset uplifting of the F-layer over the dip equator [*Farley et al.*, 1986]. On the other hand *Devasia et al.* [2002] showed that equatorward winds are a must for ESF to appear in the ionograms when the h′F is less than 300 km for the equinoctial period under consideration (March–April, 1998). The present paper attempts to critically evaluate and logically parameterize the solar activity control on the above threshold height $(h'F)_c$ so that prediction of ESF could be attempted, with a reasonable certainty.

2. Data Base and Method of Analysis

[6] During post sunset hours, the equatorial E- and the lower F-regions disappear due to recombination resulting in steep gradients (small L values) in the base of the F-region. This makes it susceptible for the R-T instability to operate. It could be seen from equation (1) that, as the ion-neutral collision frequency (ν_{in}) decreases exponentially with height, higher h′F is more favorable for ESF to occur. Ionospheric data from Trivandrum corresponding to ESF events have been collected for the equinoctial periods mostly of March–April, 1993–1998. Figure 1 depicts the F10.7 cm solar flux and h′F just before the onset of ESF as bottomside range spread, which in all the cases was between 1900–1930 LT. We have chosen the equinoctial period for the present study because of the favorable conditions for ESF occurrence over Indian longitudes [*Rastogi*, 1980]. The magnetic equator being parallel to the geographic equator at these longitudes, during equinoctial periods the sunset terminator passes through the conjugate E-regions, simultaneously releasing the F-region dynamo to become active [*Tsunoda*, 1985]. The resultant post sunset F-region rise makes the situation conducive for ESF occurrence. From the figure, one could clearly decipher the trend of h′F to increase with F10.7 cm flux. However, the variation in the base height (h′F) for a given solar flux could be as large as ~150 km. In a similar study on equatorial plasma bubbles using DMSP satellite data over a full solar cycle *Huang et al.* [2002] reported that, the base height during low solar activity could be lower by more than 100 km than the corresponding high solar activity periods. Such variations in the base height of F-region would have a say in the growth rate of the R-T instability. Since Figure 1 defies any reasonable formulation of the effect of the solar activity, certain constraints may have to be imposed on the observed h′F, like identifying a critical height $(h'F)_c$ before establishing a relation with F10.7 cm flux. Following the approach of *Devasia et al.* [2002] this critical height $(h'F)_c$ is defined as that height at which ESF would occur irrespective of the polarity of the meridional winds. The rationale for this approach is discussed later.

[7] We have used the h′F values from the ionograms obtained every 15 minutes simultaneously from the Indian stations, Trivandrum and Sriharikota during 1800–0600 h (next day), for the years 1993–1998. The meridional winds were derived following the method of *Krishnamurthy et al.* [1990]. The basic assumption is that, over the dip equator, the F layer movements are essentially due to $E \times B$ effect and at a location slightly away from the equator like Sriharikota, meridional winds (U) also have a say in it in addition to diffusion. The vertical drift velocities V_D are initially derived from the time derivative of h′F. The electrodynamical component could be obtained from $V_D = V_0 - \beta H$ where β is the effective recombination coefficient and H is the scale length given by $H = \left(\frac{1}{N}\frac{dN}{dh}\right)^{-1}$. N represents the electron density and βH the correction for the apparent change in height due to chemical recombination. This method of deriving meridional winds had been validated by vapour release experiments from Sriharikota [*Sekar and Sridharan*, 1992]. The actual meridional wind has been estimated after correcting for the chemical loss and diffusion over both the stations

$$U = \left[\frac{2(V_D \cos I - V)}{\sin 2I}\right] - W_D \tan I \qquad (2)$$

where V_D is the F-region plasma drift over Trivandrum and V that over Sriharikota. In equation (2) 'I' represents the dip angle, W_D the plasma drift velocity due to the gravitational force associated with diffusion and given by g/ν_{in}.

[8] Generally, since the uncertainty in the determination of h′F is ±15–20 km during spread F conditions, the estimated meridional winds will have an uncertainty of ±40–50 ms^{-1}. Under normal circumstances the overall accuracy taking into account the chemical loss and diffusion is estimated to be better than ±25 ms^{-1} [*Krishnamurthy et al.*, 1990]. In the present study, we consider the polarity of the winds just before the onset of ESF in the Ionograms and not later than that, and hence the uncertainties are at their minimum.

[9] The meridional wind velocities corresponding to the post sunset F-region heights (h′F) of each of the ESF events have been obtained. The estimated winds (small dots) along with the h′F as seen in the ionograms just before the onset of

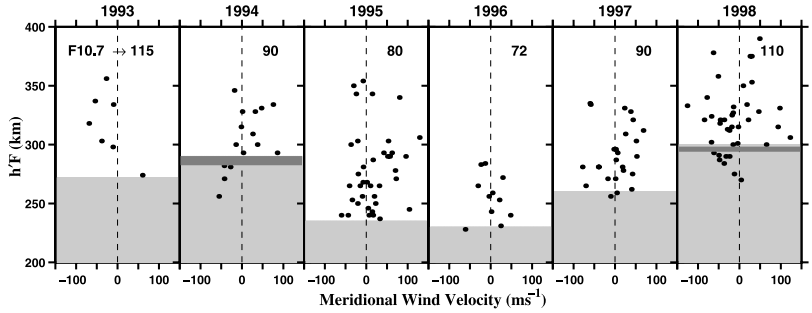

Figure 2. Variations of thermospheric meridional wind (poleward positive), just before the onset of bottomside range spread F with h′F for the equinoctial periods of 1993–1998. A significant solar cycle variation of the critical $(h'F)_c$ (denoted by the shaded area in the panel corresponding to each year) is clearly seen along with the corresponding average F10.7 cm flux.

ESF are depicted in Figure 2 for the periods under consideration. It may be noted that the meridional wind could be positive (poleward) or negative (equatorward) and the h′F shows a large variability with a span of even 150 km in certain years. The wind magnitudes also show large variation of ±100 ms^{-1}. The criterion for ESF occurrence irrespective of the polarity of meridional winds has been applied to h′F in order to determine a threshold or critical height $(h'F)_c$ below which equatorward wind is a must.

[10] The above criterion provides the important linkage between the phenomenon of Equatorial Ionization Anomaly (EIA) and the bottom side ESF. It had been shown earlier by *Raghavarao et al.* [1987], that strong EIA is a precursor to ESF. Later on *Sridharan et al.* [1994], and *Mendillo et al.* [2001] confirmed this using day glow, and TEC measurements respectively. However, the physical process by which these two phenomena are linked remained unexplained. *Raghavarao et al.* [1993] highlighted the presence of vertical winds (upward at the EIA crest and downward at the trough locations) using DE-2 data, associated with the Equatorial Temperature and Wind Anomaly (ETWA) and conjectured that these should be part of a circulatory cell converging over the magnetic equator. In another exercise, *Sekar and Raghavarao* [1987] had highlighted the role of vertically downward winds in the R-T instability. The meridional winds estimated in the present exercise, presumably set up due to ETWA fill up the gap with the equatorward wind implying downward wind over the magnetic equator. Since the period under consideration is equinoctial, there would be hardly any transequatorial flow and even when one encounters a distinct summer and winter hemispheres, the wind magnitudes are only nominal (10–20 ms^{-1}) from the summer to winter hemisphere. Therefore the large magnitude meridional winds have to be due to other factors like ETWA, and/or gravity waves. In the presence of an additional supporting factor like the downward wind, ESF could occur even with a lower h′F. *Sekar and Raghavarao* [1987] have clearly demonstrated that at a height of 300 km a vertical wind of just 16 ms^{-1} could be as effective as that of gravity itself. The vertical wind effects have been demonstrated through several nonlinear numerical simulation studies as well [*Sekar et al.*, 1994]. Once triggered, the R-T instability grows nonlinearly and a hierarchy of instabilities operates resulting in the generation of the observed irregularity spectrum. Therefore, for solar activity dependence, the possible role of additional destabilizing agencies like vertical winds should be separated out. Keeping this logic in mind, the critical height of $(h'F)_c$ is defined as that height above which ESF could occur irrespective of the polarity of the meridional winds. In the year 1993 (F10.7–115), the meridional wind had been dominantly equatorward except on one occasion. The $(h'F)_c$ then has to be below 275 km and this incidentally is the upper bound. Since we have data for one more year (1998) with nearly the same solar flux and a clear demarcation of $(h'F)_c$, the 1993 upper bound value could be taken as representative of this period. The number of data points is rather limited during this year, for want of simultaneous ionospheric data from Trivandrum and Sriharikota.

[11] The $(h'F)_c$ for every year is shown by the limits of the shaded area in each panel. The average F10.7 cm flux over the days of ESF (this average value of flux is found to be matching with the average F10.7 cm flux over the equinoctial period of the respective years) is also mentioned. The (h′F)c is clearly demarcated for the year 1994. On the other hand for 1995, the identified $(h'F)_c$ is only the upper bound. During 1996 and 1997 we have at least one event enabling the identification of $(h'F)_c$ with reasonable certainty. While for 1998, there is no ambiguity. The limitations are essentially due to the lack of data points. Figure 3 depicts the variation of the critical height $(h'F)_c$ with the average F10.7 cm flux. No doubt this linearity

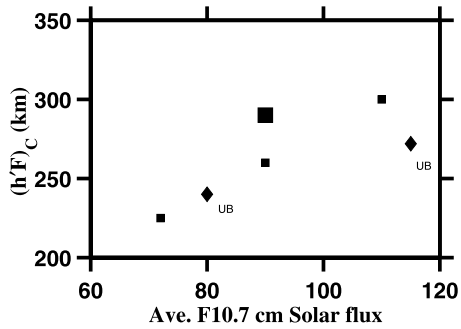

Figure 3. Relation between $[(h'F)_c]$ and solar activity represented by the average F10.7 cm solar flux. Wherever clear-cut demarcation is not possible the upper or lower bound has been indicated by a different symbol (◆). The uncertainties in $h'F_c$ lie within the size of the respective symbols.

would get affected since at least in a couple of years the $(h'F)_c$ is only the lower or upper bounds. In spite of this limitation, the critical height concept emerges as a useful parameter in the light of Figure 1. This also implies that for a given solar activity level, if the (h′F) is above the critical height given by Figure 3 during post sunset hours i.e., around 1900–1930 h local time, there exists a very high probability of bottom side ESF occurrence. Once triggered, as mentioned earlier, the instability grows nonlinearly enabling a hierarchy of instabilities to take over. The nonlinear growth and also sustenance of ESF will now be decided by the background ionospheric conditions like the maximum electron density (N_{max}), the topside gradient in the electron density (N_e) profile etc., manifesting itself in its varied forms. The present results enable the formulation of the solar activity effects and take us closer towards a better understanding of the day-to-day variability of the bottomside Equatorial Spread F.

[12] **Acknowledgments.** The reported results are an outcome of the studies of Working Group III of Indian Solar Terrestrial Energy Program (ISTEP) on Ionosphere-Thermosphere-Magnetosphere interactions. The Dept. of Science and Technology had been the nodal agency and the basic support for this work is from Department of Space, Government of India. The authors wish to acknowledge the critical observations by the referees which had improved the clarity of the presentation.

References

Aarons, J. (1993), The longitudinal morphology of equatorial F layer irregularities relevant to their occurrence, *Space Sci. Rev.*, *63*, 209–243.

Abdu, M. A. (2001), Outstanding problems in the equatorial ionosphere-thermosphere electrodynamics relevant to spread F, *J. Atmos. Sol. Terr. Phys.*, *63*, 869–884.

Abdu, M. A., J. A. Bittencourt, and I. S. Batista (1981), Magnetic declination control of the equatorial F region dynamo electric field development and spread F, *J. Geophys. Res.*, *86*, 11,443–11,446.

Abdu, M. A., I. S. Batista, and J. H. A. Sobral (1992), A new aspect of magnetic declination control of equatorial spread F and F region dynamo, *J. Geophys. Res.*, *97*, 14,897–14,904.

Basu, S., and B. Coppi (1999), Relevance of plasma and neutral wind profiles to the topology and the excitation of modes for the onset of the equatorial spread F, *J. Geophys. Res.*, *104*, 225–232.

Chandra, H., and R. G. Rastogi (1972), Equatorial spread F over a solar cycle, *Ann. Geophys.*, *28*, 709–716.

Devasia, C. V., N. Jyoti, K. S. Viswanathan et al. (2002), On the plausible linkage of thermospheric meridional winds with equatorial spread F, *J. Atmos. Sol. Terr. Phys.*, *64*, 1–12.

Farley, D. T., E. Bonelli, B. G. Fejer, and M. F. Larsen (1986), The prereversal enhancement of the zonal electric field in the equatorial ionosphere, *J. Geophys. Res.*, *91*, 13,723–13,728.

Fejer, B. G., and M. C. Kelley (1980), Ionospheric irregularities, *Rev. Geophys.*, *18*, 401–454.

Fejer, B. G., L. Scherliess, and E. R. de Paula (1999), Effects of the vertical plasma drift velocity on the generation and evolution of equatorial spread F, *J. Geophys. Res.*, *104*, 19,859–19,869.

Hanson, W. B., B. L. Cragin, and A. Dennis (1986), The effect of vertical drift on the equatorial F region stability, *J. Atmos. Terr. Phys.*, *48*, 205–212.

Huang, C. Y., W. J. Burke, J. S. Machuzak et al. (2002), Equatorial plasma bubbles observed by DMSP satellites during a full solar cycle: Toward a global climatology, *J. Geophys. Res.*, *107*(A12), 1434, doi:10.1029/2002JA009452.

Hysell, D. L., and J. Burcham (2002), Long term studies of equatorial spread F using the JULIA radar at Jicamarca, *J. Atmos. Terr. Phys.*, *64*, 1531–1543.

Kelley, M. C. (1989), *The Earth's Ionosphere: Plasma Physics and Electrodynamics*, Academic, San Diego, Calif.

Krishnamurthy, B. V., S. S. Hari, and V. V. Somayajulu (1990), Nighttime equatorial thermospheric meridional winds from h′F data, *J. Geophys. Res.*, *95*, 4307–4310.

Maruyama, J. (1988), A diagnostic model for equatorial spread F: 1. Modal description and application to electric fields and neutral wind effects, *J. Geophys. Res.*, *93*, 14,611–14,622.

Mendillo, M., J. Baumgardner, P. Xiaoquing et al. (1992), Onset conditions for equatorial spread F, *J. Geophys. Res.*, *97*, 13,865–13,876.

Mendillo, M., J. Meriwether, and M. Biondi (2001), Testing the thermospheric neutral wind suppression mechanism for day-to-day variability of equatorial spread F, *J. Geophys. Res.*, *106*, 3655–3663.

Raghavarao, R., S. P. Gupta, R. Sekar et al. (1987), In situ measurements of winds, electric fields and electron densities at the onset of equatorial spread-F, *J. Atmos. Terr. Phys.*, *49*, 485–492.

Raghavarao, R., W. R. Hoegy, N. W. Spencer, and L. E. Wharton (1993), Neutral temperature anomaly in the equatorial thermosphere: A source of vertical winds, *Geophys. Res. Lett.*, *20*, 1023–1026.

Rastogi, R. G. (1980), Seasonal variation of equatorial spread-F in the American and Indian zone, *J. Geophys. Res.*, *85*, 722–726.

Sahai, Y., P. R. Fagundes, and J. A. Bittencourt (2000), Transequatorial F-region ionospheric plasma bubbles: Solar cycle effects, *J. Atmos. Sol. Terr. Phys.*, *62*, 1377–1383.

Sastri, J. H., B. S. Murthy, and K. Sasidharan (1979a), Range and frequency spread F at Kodaikanal, *Ann. Geophys.*, *35*, 153–158.

Sastri, J. H., K. Sasidharan, V. Subrahmanyam, and M. Sriramarao (1979b), Seasonal and solar cycle effects in the occurrence of equatorial spread F configurations, *Ind. J. Radio Space Phys.*, *8*, 135–138.

Sastri, J. H., R. Sridharan, and T. K. Pant (2004), Equatorial ionosphere-thermosphere system during geomagnetic storms, in *Disturbances in Geospace: The Storm-Substorm Relationship*, *Geophys. Monogr. Ser.*, vol. 142, edited by A. Surjalal Sharma, Y. Kamide, and G. S. Lakhina, pp. 185–203, AGU, Washington, D. C.

Sekar, R., and R. Raghavarao (1987), Role of vertical winds on the Rayleigh-Taylor instabilities of the night time equatorial ionosphere, *J. Atmos. Terr. Phys.*, *49*, 981–985.

Sekar, R., and R. Sridharan (1992), Validity of the estimates of nighttime meridional winds made from bottomside ionogram, *J. Atmos. Terr. Phys.*, *54*, 1197–1199.

Sekar, R., R. Suhasini, and R. Raghavarao (1994), Effects of vertical winds and electric fields in the nonlinear evolution of equatorial spread F, *J. Geophys. Res.*, *99*, 2205–2213.

Sridharan, R., D. P. Raju, R. Raghavarao, and P. V. S. Ramarao (1994), Precursor to equatorial spread-F in OI 630.0 nm dayglow, *Geophys. Res. Lett.*, *21*, 2797–2800.

Subbarao, K. S. V., and B. V. Krishnamurthy (1994), Seasonal variations of equatorial spread F, *Ann. Geophys.*, *12*, 33–39.

Sultan, P. J. (1996), Linear theory and modeling of the Rayleigh-Taylor instability leading to the occurrence of equatorial spread F, *J. Geophys. Res.*, *101*, 26,875–26,891.

Tsunoda, R. T. (1985), Control of the seasonal and longitudinal occurrence of equatorial scintillations by the longitudinal gradient in integrated F region Pederson conductivity, *J. Geophys. Res.*, *90*, 447–456.

Woodman, R. F., and C. LaHoz (1976), Radar observations of F region equatorial irregularities, *J. Geophys. Res.*, *81*, 5447–5466.

C. V. Devasia, N. Jyoti, R. Sridharan, and D. Tiwari, Space Physics Laboratory, Vikram Sarabhai Space Centre, Trivandrum, 695022, India. (r_sridharan@vssc.org)